

Evaluation of the relationship between the main lineament trends and the geometry of the drainage network using SPOT-5 and SRTM data: a case study from Bulghah area, Saudi Arabia

Ahmed Madani^{1,2} · Burhan Niyazi³

Received: 25 August 2014 / Accepted: 15 April 2015 / Published online: 12 May 2015
© Saudi Society for Geosciences 2015

Abstract This paper aims to evaluate the relationship between lineament trends and drainage network orientations at Bulghah area, Saudi Arabia, using SPOT-5 and Shuttle Radar Topography Mission (SRTM) elevation data. Three sectors namely A, B, and C represent the study area. They are covered by Hulayfah volcanics intruded by diorite intrusion, and they are traversed by numerous lineaments of various directions and lengths. Lineaments and drainage network distribution maps are generated using panchromatic SPOT-5 imagery and SRTM data, respectively. Rose diagrams for lineaments and drainage lines are constructed to demonstrate the main azimuth trends dominated in each sector. The results of the present study revealed the presence of a strong and a close relationship between lineament trends and drainage network orientations. Most of the drainage channels are structurally controlled, and they are following Nabitah and Najd fault directions. At sectors “A” and “C,” the drainage networks are completely coincide with the major lineaments having NW–SE, NE–SW, and E–W directions. At sector “B,” the N–S to NNE Nabitah older strike–slip fault has been offsetted by NW–SE Najd fault system. Lineament density map for the study area is generated using lineaments lengths (km) to locate the most promising areas for groundwater exploration. This

study presents two promising sites for groundwater exploration at sectors A and C.

Keywords Lineament–drainage relationship · SPOT-5 · SRTM · Bulghah area, Saudi Arabia

Introduction

Linear features on the earth surface attract the attention of many scientists in the field of geology since early 20th century (Hobbs 1904; O’Leary et al. 1976; Zakir et al. 1999). The first usage of the term “linear” is probably utilized by Hobbs (1904) to refer the linear feature on the earth surface. O’Leary et al. (1976) defined the lineament as a mappable, simple, or composite linear feature of a surface whose parts are aligned in a rectilinear or slightly curvilinear relationship and which differ from the pattern of adjacent features and presumably reflect some subsurface phenomenon. Sabins (1997) used the term “lineament” to refer to any linear feature on the earth’s surface that reflects an underlying geological structure such as fault, fracture, or joints. Satellite imageries and aerial photos are usually utilized for lineament extraction either manually or through automated processes. Moderate spatial resolution satellite data (e.g., Landsat and Advanced Spaceborne Thermal Emission and Reflection Radiometer (ASTER)) imageries are commonly used for lineament extraction (Madani 2009). Radarsat and Shuttle Radar Topography Mission (SRTM) elevation data are also utilized to recognize and delineate the topographic lineaments (Masoud and Koike 2011). High-spatial-resolution panchromatic imageries such as Ikonos and QuickBird are used for linear feature extraction. Lineament mapping is an important issue for many geological applications such as (i) selection of the optimum wavelengths used for automatic lineament extraction (Madani 2002), (ii)

✉ Ahmed Madani
aamadani18@hotmail.com

¹ Water Research Center, King Abdulaziz University, PO Box 80200, Jeddah 21589, Saudi Arabia

² Geology Department, Faculty of Science, Cairo University, Giza, Egypt

³ Faculty of Meteorology, Environment and Arid Land Agriculture, King Abdulaziz University, Jeddah, Saudi Arabia

utilization of ASTER panchromatic band for lineament extraction and studying their relationship to mineral locations (Madani and Emam 2011), (iii) study of the lineament characterization and their tectonic significant (Solomon and Ghebream 2006), (iv) drainage network geometry versus tectonic elements (Musumeci et al. 2003; Hodgkinson et al. 2006; Ribolini and Spagnolo 2008), and (v) lineament

analyses for assessment of groundwater potential (Anudu et al. 2011). This study aims to (i) evaluate the relationship between the lineament trends and the drainage network geometry at Bulghah area, Saudi Arabia, using panchromatic SPOT-5 imagery and SRTM elevation data and (ii) locate the most promising sites for groundwater targeting at the study area.

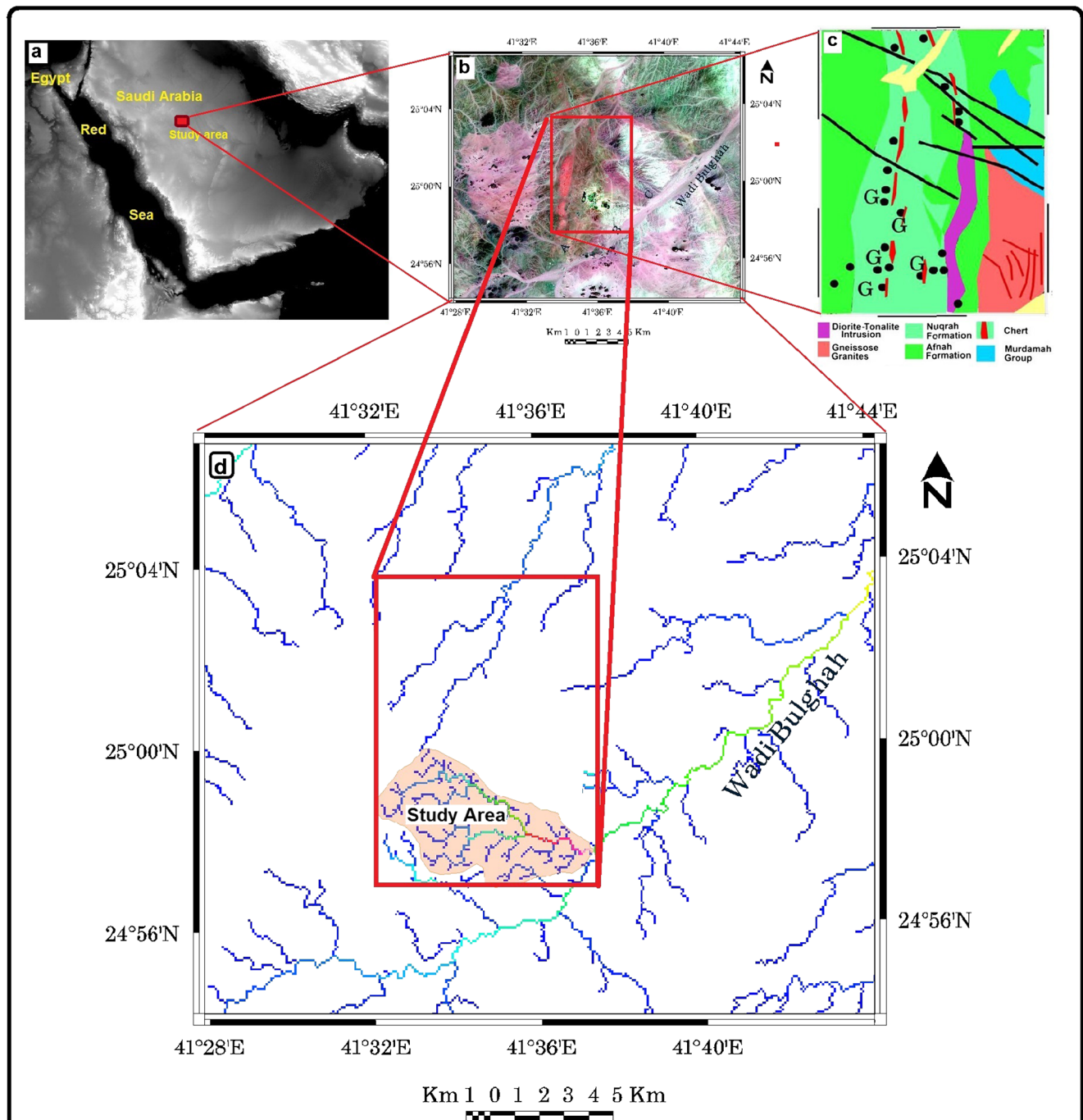


Fig. 1 Study area location. **a** Saudi Arabia. **b** SPOT-5 false color composite 4, 3, and 2 in RGB imagery. **c** Geological map for the study area modified after Delfour (1977). **d** The entire drainage network at Wadi Bulghah area

Study area

Initial examination of the false color composite SPOT-5 imagery helps greatly in defining the study area (Fig. 1a, b). We have selected the southwestern part of the Bulghah gold mine area, Saudi Arabia, to test the purposes of this study. The study area lies approximately 520 km west of Riyadh city, the capital of Saudi Arabia. It is divided into three sectors namely A, B, and C (Fig. 2). In each sector, we are dealing with the main lineament trends and the drainage network geometry. Sector “A” is the upstream part of many small wadies that strike in NW–SE direction and drained in SE direction crossing sectors “B and C” toward the main channel of Wadi Bulghah which has NE–SW strike (Fig. 1d). These wadies are traversed through different rock units such as Hulayfah volcanics, diorite intrusion, and alkali granites. The oldest rock unit exposed at the study area is represented by Hulayfah volcanics. They are made up of the older Afna Formation and the younger Nuqrah Formation. They are intruded by N–S fault-bounded diorite intrusion (Fig. 1c; Delfour 1977). Harbi and Madani (2014) presented a new geological map for the study area based on field data and fusion of SPOT-5 data. The study area is important for gold production. It contains Bulghah gold mine and Bulghah North deposit. Gold production at the Bulghah mine started on 2002 and reached 1.735-t tonnage with 0.7 g/t Au in 2007 (SRC 2007). Water is an important issue used to perform several mining activities at Bulghah gold mine. The present study aims to locate the most promising groundwater potential sites. It will provide decision makers at Bulghah mine with right location to look for groundwater.

Regional geology

Figure 1c represents a simplified geological map for the study area modified after Delfour (1977). The country rocks are represented by Hulayfah volcanics which consist of Nuqrah

Formation and Afna Formation. The older Afna Formation occurs mainly in the western part of the study area and is made up of andesitic volcanic rocks and volcanoclastic derivatives. Nuqrah Formation consists of acidic volcanoclastic rocks. Discontinuous ridges of gossans are exposed at sector “B” and are distinguished on FCC SPOT imagery by their red image signature (Fig. 2). Discontinuous marble bands forming nearly N–S to NNW trending ridges are exposed at sector “C” to the east of the diorite intrusion. They are commonly occurring within the middle part of Nuqrah Formation.

Hulayfah volcanics are unconformably overlain by Murdama Group which is represented by rhyolite, andesite, sandstone, conglomerate, and marble. Diorite and alkali granite intrusions belonging to Idah (620–615 Ma) and Abanat (585–570 Ma) suites are intruded in the previously described rock units.

Materials and methods

SPOT-5 panchromatic imagery (5-m spatial resolution) and SRTM elevation data are the main remote sensing data used throughout this study for lineament extraction and drainage network derivation. Integration of the processed remote sensing and field data is used to clarify the relationship between the lineament trends and the drainage network orientations at the study area. Many authors utilized digital satellite data for automatic lineament extraction using the following: (i) directional filtering, nonlinear, and morphological spatial filters (Süzen and Toprak 1998; Wahby et al. 2001); (ii) edge enhancement algorithms and linking methods (Koike et al. 1995); and (iii) Fourier transformation and knowledge-based systems (Morris 1991). LINE module (Geomata package) is used to extract lineaments automatically by performing the following: (i) edge detection, (ii) threshold, and (iii) linear feature extraction steps. The extraction process is performed under user-defined parameters including the following: (i)

Fig. 2 A 3-D perspective view showing locations of A, B, and C sectors

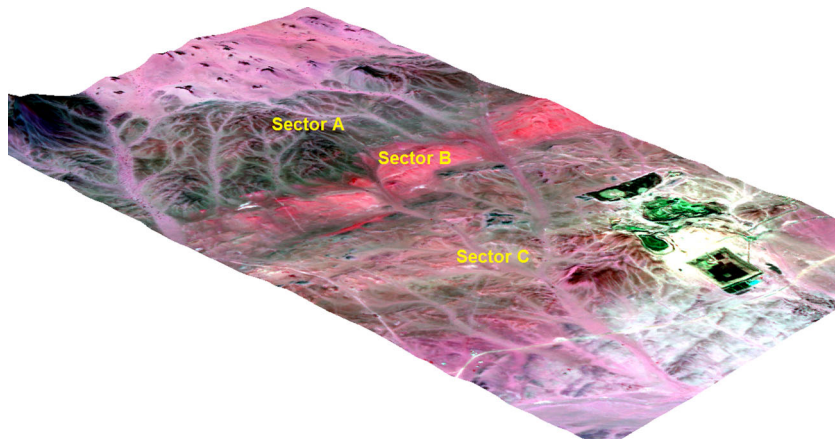
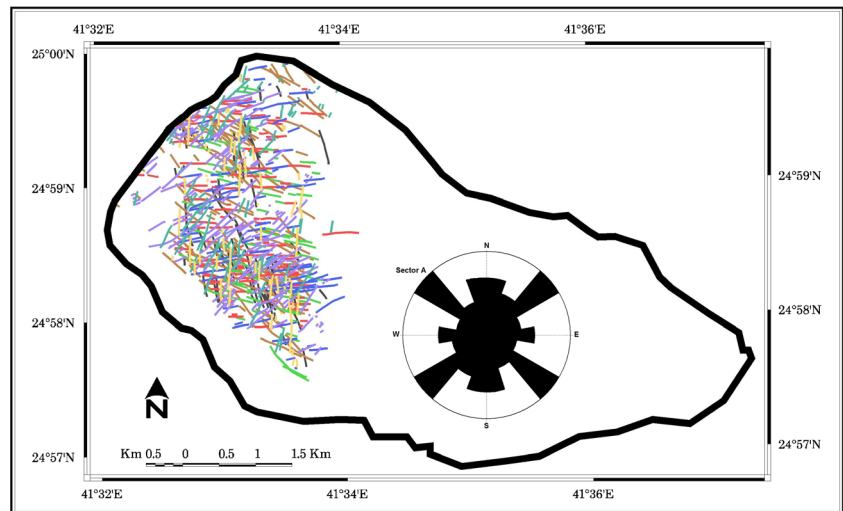


Fig. 3 The main lineament trends extracted automatically over sector “A” using panchromatic SPOT-5 imagery with their lineament frequency rose diagram



edge filter radius=5, (ii) minimum edge gradient=20, (iii) minimum line length=5, (iv) line fitting tolerance=3, (v) maximum angular difference=15, and (vi) maximum linkage difference=50. In the first step, edge detection algorithm is applied to produce an edge strength image. Panchromatic SPOT-5 imagery is filtered with a Gaussian function and radius equal to 5. In the second step, the edge strength image is thresholded using value equal to 20 to obtain a binary image. Each ON pixel of the binary image represents an edge element. In the third step, lineaments are extracted from the binary edge image. This step consists of several substeps. First, a thinning algorithm is applied to the binary edge image to produce pixel-wide skeleton lines. Then, a sequence of pixels for each line is extracted from the image. Any line with the number of pixels less than 5 is discarded from further processing. An extracted pixel line is converted to vector form by fitting piecewise line segments to it. The resulting polyline is an approximation to the original pixel line where the maximum fitting error is 3. Finally, the LINE algorithm links pairs of

polylines which satisfy the following criteria: (1) two end segments of the two polylines face each other and have similar orientation (the angle between the two segments is less than 15) and (2) the two end segments are close to each other (the distance between the end points is less than 50). This method failed to differentiate between geological and nongeological linear features. Manual editing is used to eliminate the nongeological linear features and to enhance the results. The rest of lineaments which represent the geological structures are recorded in vector segment used later for statistical analyses and rose diagram construction.

Drainage network for the study area is generated automatically from 90-m resolution SRTM digital elevation data using Geomatica software. Two drain modules are used. The first module (DWCON) produces four data sets which are as follows: (i) depression-less digital elevation data, (ii) flow direction for each pixel, (iii) a flow accumulation data set in which each pixel receives a value equal to the total number of cells that drain to it, and (iv) a delta value data set in which each

Fig. 4 The main trends of the drainage lines over sector “A” digitized from the drainage network with their drainage frequency rose diagram

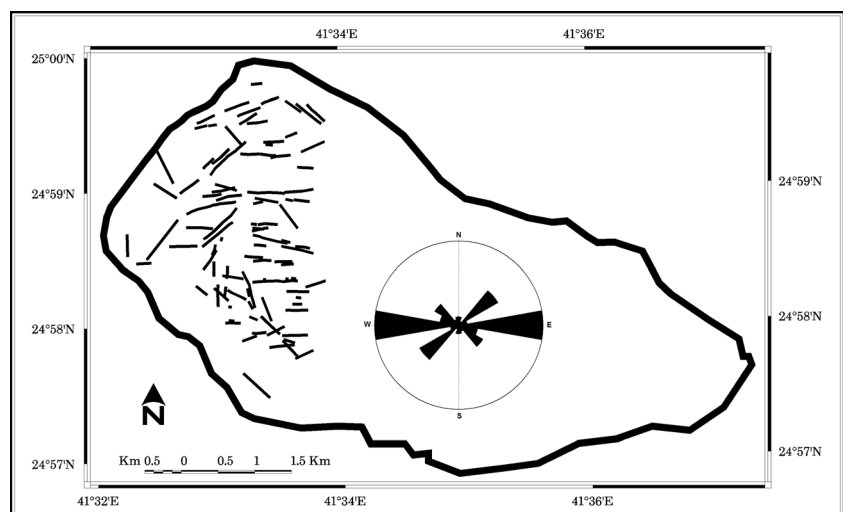
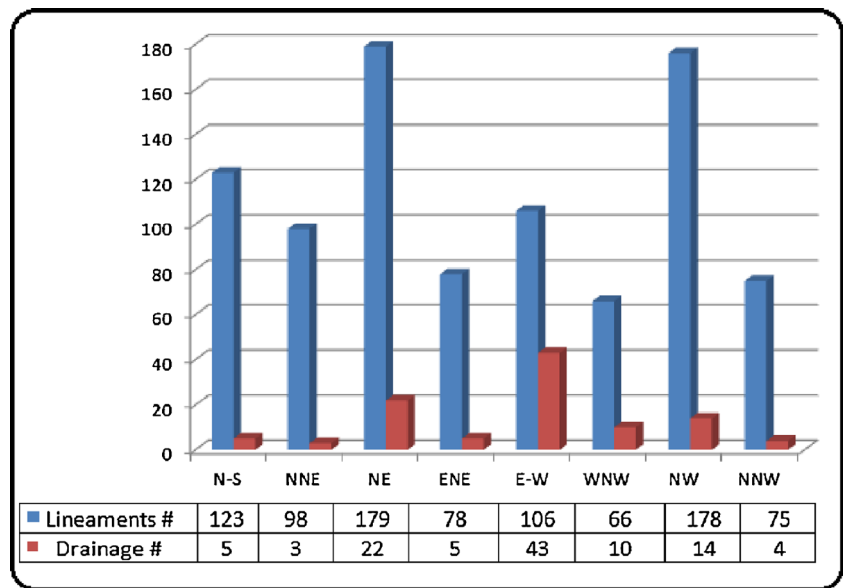


Fig. 5 Histograms comparing the frequencies of the directional trends of lineaments and drainage over sector “A”



pixel equals the increase in flow accumulation value in the flow direction. DRAIN module is used later to generate the drainage network layer using the flow accumulation data. Vector layer for drainage network orientations is generated and used for statistical analyses and rose diagram construction.

Results

Sector A

Sector A constitutes the upstream part of the study area (Fig. 2). It is characterized by slightly elevated hills dissected by small channels draining mainly toward the SE direction. Parallel and subparallel drainage patterns are predominant in this sector. Rock units that exposed at sector A are made of Nuqrah

Formation. They are made up of acidic volcanoclastic rocks including agglomerate, fine-laminated tuffs, and intercalations of jasper and cherty tuffs. It is clearly observed that the structural elements especially faults are the main controlling factor affecting the drainage network orientations in this sector.

Figure 3 shows the main trends of the automatically extracted lineaments over sector A using panchromatic SPOT-5 band with their rose diagram. The main lineament trends are NE–SW and NW–SE constituting the 19.86 and 19.53 %, respectively. The second major trends recorded in sector A are N–S and E–W which constitute 13.65 and 11.76 %, respectively. ENE–WSW, NNW–SSE, and WNW–ESE are subordinate directions constituting 8.65, 8.32, and 7.32 % of total lineament number, respectively. The lineament frequency rose diagram shows the high degree of preferred orientation in the conjugate systems NE–SW and NW–SE, and N–S and E–W directions.

Fig. 6 The main lineament trends extracted automatically over sector “B” using panchromatic SPOT-5 imagery with their lineament frequency rose diagram

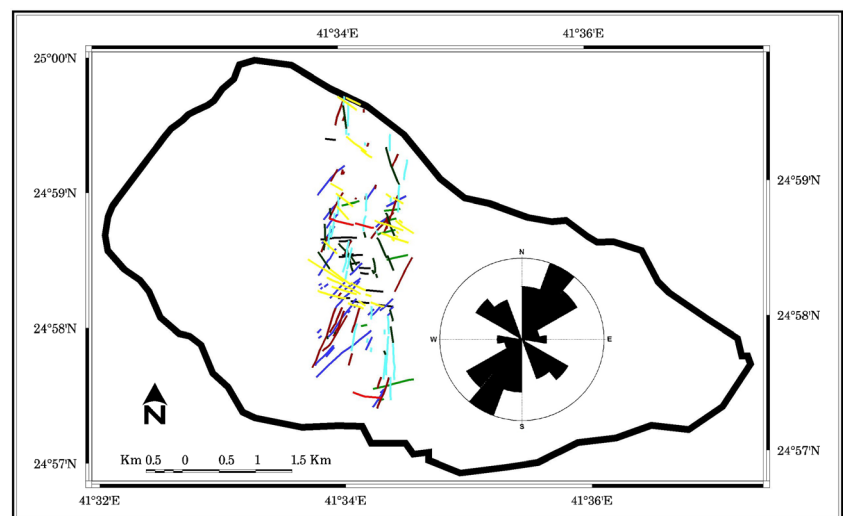


Fig. 7 The main trends of the drainage lines over sector “B” digitized from drainage network with their drainage frequency rose diagram

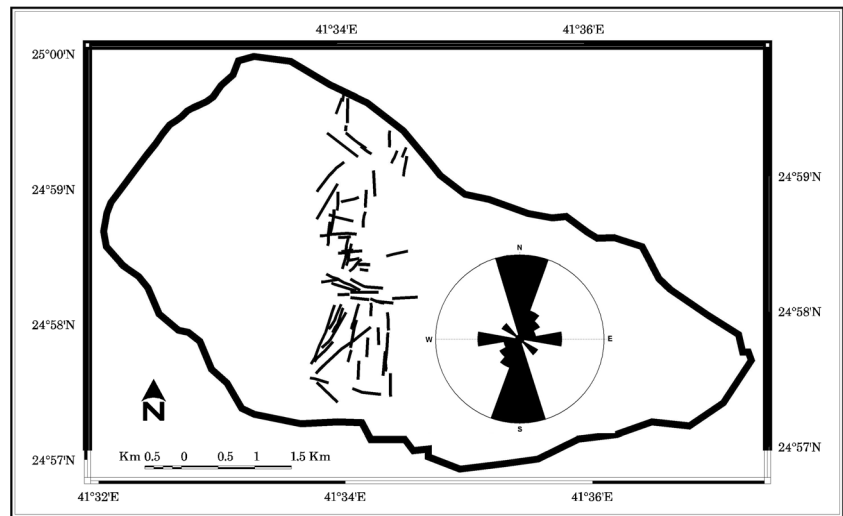


Figure 4 shows the drainage lines digitized from SRTM-derived drainage network for sector A. The rose diagram shows the preferred orientations along NE–SW and NW–SE conjugate system with high frequency in E–W trend. Visual inspection of high-spatial-resolution SPOT-5 imagery revealed the presence of many small E–W drainage channels drained toward the east direction. These channels are responsible for the high E–W drainage frequency.

The histograms comparing the frequencies of the directional trends of lineaments and drainage over sector A are shown in Fig. 5. Both lineament lines and drainage pattern are dominated by NE–SW and NW–SE trends, as indicated by their numbers (179 and 176: lineaments; 22 and 14: drainage) and lengths (35.5 and 41.6 km: lineaments; 7.2 and 4.3 km: drainage). The second fracture systems observed at the study area are N–S and E–W trends.

Sector B

Sector B is the most distinguished sector on the FCC SPOT-5 imagery (Fig. 2). It has a red image signature. It is characterized by plain area with some scattered gossan ridges (Nuqrah Formation) aligned in N–S direction. It is dominated by several NW–SE offsets. In this sector B, the main lineament trend is N–S to NNE (Fig. 6). It constitutes 39.7 % of the total lineament number. The conjugate system NE–SW and NW–SE is also observed and found that they constitute 18.49 and 15.60 % of the total lineament number, respectively. Lineament frequency rose diagram shows the high degree of preferred orientation in the NE–SW, NW–SE, and N–S to NNE trends. Figure 7 shows the drainage lines digitized from drainage network for sector B. They are frequently oriented in N–S and E–W directions representing 39.02 and 19.51 % of total digitized drainage lines. Figure 8 shows the histograms

Fig. 8 Histograms comparing the frequency of the directional trends of lineaments and drainage cover sector “B” area

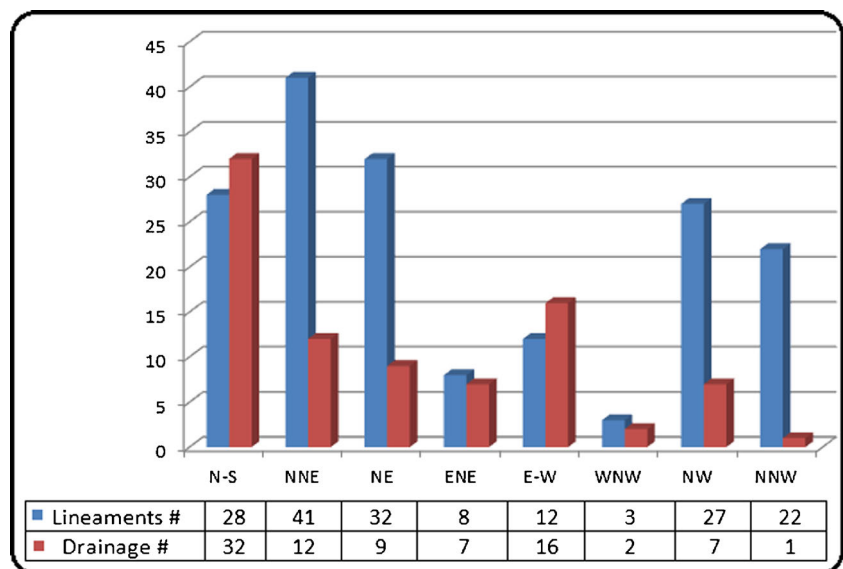
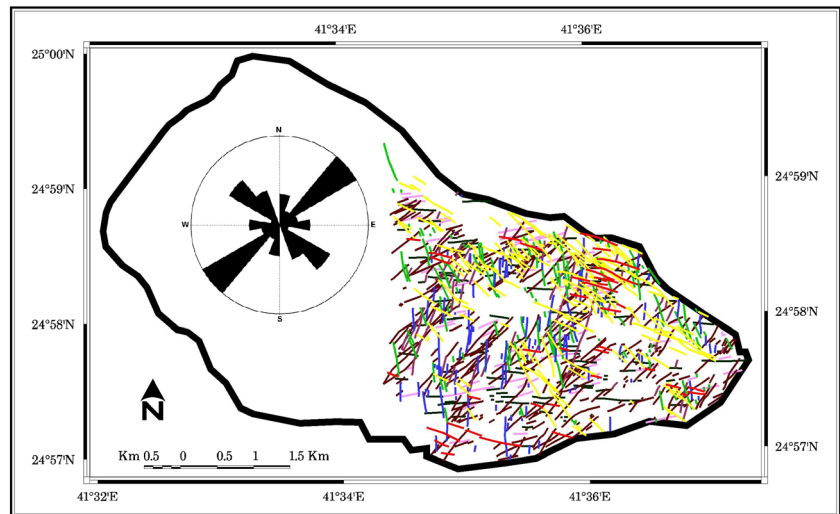


Fig. 9 The main lineament trends extracted automatically over sector “C” using panchromatic SPOT-5 imagery with their lineament frequency rose diagram



comparing the frequency of the directional trends of lineaments and drainage cover sector B area. When lump, the N–S and NNE lineaments and drainage numbers, we can conclude that

1. N–S to NNE trends are the main directions for both lineaments and drainage networks as indicated by their numbers (69 and 44) while their lengths are 15 and 11.6 km, respectively.
2. NE–SW and NW–SE trends occupied the second rank.

Sector C

It contains large varieties of rock units. It is covered by Hulayfah volcanics, marble ridges, diorite, and alkali granite intrusions. Small wadies having NW and E–W trends are traversing these rock units. They drain east toward the main channel of Wadi Bulghah which has

NE–SW strike. The area is characterized by presence of several dike swarms having different orientations. Figure 9 shows the main trends of the automatically extracted lineaments over sector C using panchromatic SPOT-5 band. The main lineament trends are NE–SW and NW–SE constituting 29.68 and 19.22 % of total number, respectively. The second major trends recorded at sector C are N–S and E–W which constitute 10.75 and 10.85 % of total number, respectively. The lineament frequency rose diagram shows the high degree of preferred orientation in the conjugate directions NE–SW and NW–SE, and N–S and E–W. Figure 10 shows the drainage lines digitized from SRTM-derived drainage network for sector C. The rose diagram shows the high degree of preferred orientations in NE–SW and NW–NE conjugate system. Figure 11 shows the histograms comparing the frequency of the directional trends of lineaments and drainage cover sector C area. The lineament and drainage pattern of the study area is dominated by

Fig. 10 The main trends of the drainage lines over sector “C” digitized from drainage network with their drainage frequency rose diagram

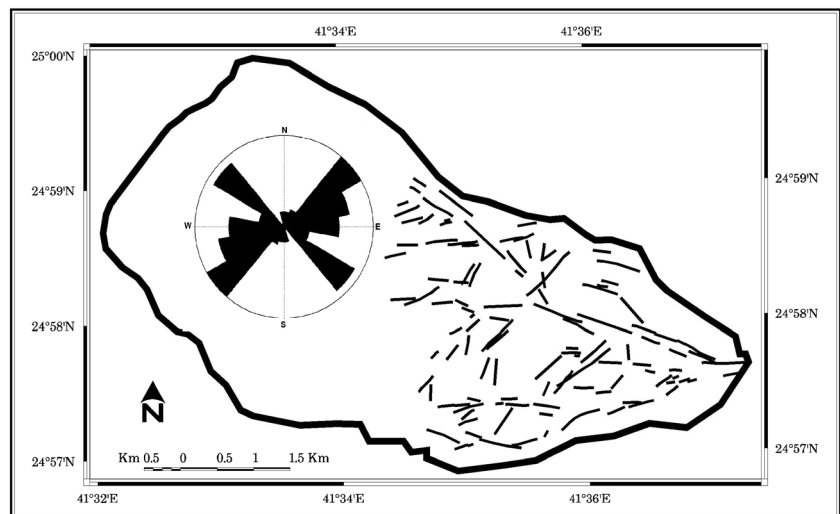
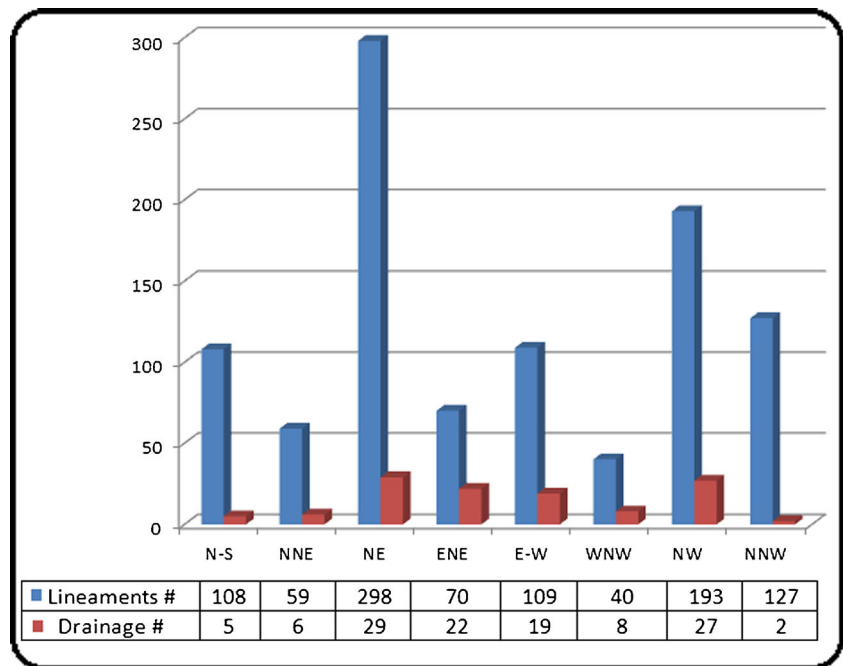


Fig. 11 Histograms comparing the frequency of the directional trends of lineaments and drainage cover sector “C” area



NE–SW and NW–SE trends, which show up in both numbers and lengths.

Field observation

Faults

Field study revealed the presence of three main fault systems observed at the study area. The first fault system is recorded at sector B and is represented by N–S left-lateral strike–slip fault following Nabitah belt trend. The second fault system observed at the study area is represented by left-lateral strike–slip Najd fault system trend in NW–SE direction. The third fault trend has E–W direction. Conjugate fault system strikes in NE–SW and NW–SE directions are observed at sector C crosscutting the diorite intrusion (Fig. 12a). They are characterized by the presence of brownish hematitic clay material along the fault plane (Harbi and Madani 2014).

Dikes

Three main types of dike swarms are observed at sector C and are easily distinguished on the FCC SPOT imagery. The first type is porphyritic andesite, about 10 m thick, has NW–SE strike, and is observed at the Bulghah north open-pit site cutting diorite intrusion. The second type of dikes has N–S direction and is represented by acidic dikes cutting alkali granite (Fig. 12b). Pink acidic dikes that have NE–SW direction are also observed.

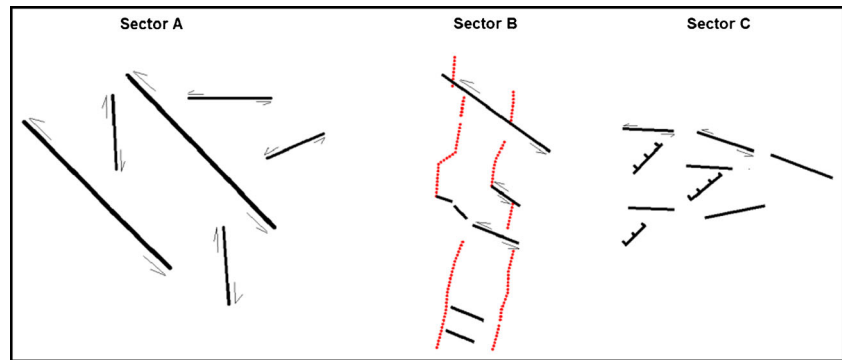
Joints

Three main joint sets are observed in the granitoid rocks exposed at sector C (Fig. 12c). They are mainly subvertical and have NE–SW, NW–SE, and N–S directions. Hybrid joint systems (extensional and shear) are also recorded at the study area.



Fig. 12 Field observations from sector “C.” **a** Conjugate faults with hybrid joint systems crosscut diorite intrusion. **b** N–S acidic dike cut through alkali granite. **c** Joint sets in granitic rocks

Fig. 13 Structural interpretation of the major lineaments at the study area



Discussion

Lineament–drainage relationships

Visual inspection of the lineaments and drainage maps as well as their rose diagrams at sectors “A, B, and C” revealed the presence of a close relationship between the main lineament trends and the drainage network orientations. Most of the drainage channels are structurally controlled by and follow Nabitah and Najd fault structures. At sectors “A and C,” the conjugate system NE–SW and NW–SE represents the main lineament trends as well as the main drainage network orientations. At sector B, the lineament trends and the drainage network orientations are completely coincide with N–S to NNE, NW–SE, and E–W directions.

Tectonic implications of the lineaments

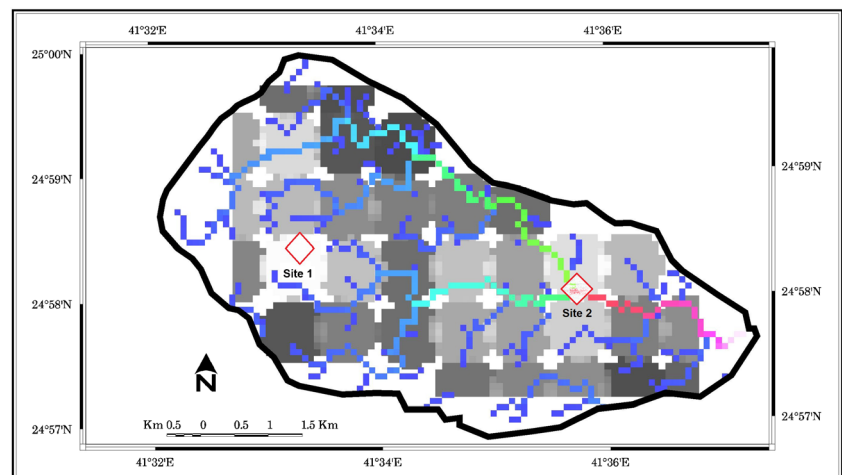
Sector B is considered as the clue of the structural history of the study area. It contains the most interesting feature observed on FCC SPOT image “strike–slip bend basin” (Fig. 2). The basin elongates in N–S direction and is dissected by NW–SE Najd faults in its southern parts. Madani (2011) studied in detail the structural elements in the study area and its relation to gold mineralization. His study revealed the presence of two main

deformational events which had affected the rock units exposed at the study area. The first deformational event is represented by N–S to NNE–SSW Nabitah fault system. Generally, Nabitah belt divided the Arabian Shield into two zones. The inner zone is characterized by sigmoidal fish-shaped shear zones whereas the outer zone is characterized by the presence of gneiss domes (Quick 1991). The older Nabitah structure has been offsetted by NW–SE Najd fault system (Figs. 2 and 13) which represents the second deformational event recorded at the study area. Najd fault system is considered as one of the most important feature crosscutting the Arabian Shield and is originated during the Najd tectonic cycle. Generally, it is approximately 300 km wide and extends more than 1000 km in NW–SE trend. It is associated with a complex array of secondary structures including strike–slip, oblique–slip, normal faults and dike swarms. The distribution of secondary structures indicates that compressional and extensional conditions are prevailing at sectors A and C, respectively (Fig. 13). These major fractures are highly susceptible to weathering and form Wadi valleys following N–S, NE–SW, NW–SE, and E–W directions.

Lineament density and groundwater exploration

In fractured aquifer, fractures play an important role in groundwater production. They act as conduits for groundwater flow.

Fig. 14 The most promising sites for groundwater targeting for the study area based on lineament density map



Several authors investigated the relationship between the lineaments and the groundwater occurrences (Lattman and Parizek 1964; Woodruff et al. 1974; Odeyemi et al. 1985; Magowe and Carr 1999; Bassey et al. 1999; Anomohanran 2013). They concluded that the groundwater accumulation and, consequently, well production increase in highly fractured areas. In this study, results of lineament extraction process show only the dimensions, directions, and spatial distribution of the lineaments over the study area. To convert this form into density form, a grid with spatial area of about 800 m² is generated and the cumulative length of lineaments (km) in each grid cell is calculated. Lineament density map (Fig. 14) is generated using density module of Geomatica package to give an idea about the concentration of lineaments in the study area. Areas having high lineament density (white and light grey colors) represent areas with relatively high groundwater potentials. Two promising sites for groundwater targeting are detected based on lineament density map. The first site lies at the intersections of NW–SE, N–S, and E–W drainage orientations at sector A, whereas the second site lies at sector C and occupies the intersection of NW–SE and E–W drainage orientations.

Conclusion

Results of the present study reveal the presence of strong and close relationship between lineament trends and drainage network orientations at Bulghah area, Saudi Arabia. Most of drainage channels are structurally controlled and follow either Nabitah structures or Najd fault system. At sectors A and C, the drainage channels are completely coincide with the lineament trends and follow NW–SE, NE–SW, and E–W directions. At sector B, the N–S to NNE and NW–SE channel systems are recorded representing Nabitah and Najd fault systems. This study utilized the lineament density map to locate the most promising locations for groundwater potentiality. A site in sector A and another one in sector C are found to be promising spots for groundwater potentiality.

Acknowledgments This work was funded by the Deanship of Scientific Research (DSR), King Abdulaziz University, Jeddah, under grant no. (123-001-D1434). The authors, therefore, acknowledge with thanks DSR technical and financial support.

References

- Anomohanran O (2013) Investigation of groundwater potential in some selected towns in Delta North District of Nigeria. *Int J Appl Sci Technol* 3(6):61–66
- Anudu GK, Onuba LN, Ufondu LS (2011) Geoelectric sounding for groundwater exploration in the crystalline basement terrain around Onipe and adjoining areas, southwestern Nigeria. *J Appl Technol Environ Sanitation* 1(4):343–354
- Bassey NE, Ezeigbo HI, Kwache JB (1999) A hydrogeological study of Duhu area (Sheet 135) NE Nigeria on the basis of aeromagnetic data. *Water Resour J NAH* 10:26–30
- Delfour J (1977) Geology of the Nuqrah quadrangle, sheet 25E. Kingdom of Saudi Arabia, D.G.M.R., Geologic Map GM-28, scale 1:200 000, 32 p
- Harbi H, Madani A (2014) Utilization of SPOT 5 data for mapping gold mineralized diorite–tonalite intrusion, Bulghah gold mine area, Saudi Arabia. *Arab J Geosci* 7:3829–3838
- Hobbs WH (1904) Lineaments of the Atlantic boarder region. *Geol Soc Am Bull* 15:483–506
- Hodgkinson JH, McLoughlin S, Cox M (2006) The influence of geological fabric and scale on drainage pattern analysis in a catchment of metamorphic terrain: Lacey's Creek, southeast Queensland, Australia. *Geomorphology* 81:394–407
- Koike K, Nagano S, Ohmi M (1995) Lineament analysis of satellite images using a segment tracing algorithm (STA). *Comput Geosci* 21(9):1091–1104
- Lattman LH, Parizek RR (1964) Relationship between fracture traces and the occurrence of groundwater in carbonate rocks. *J Hydrol* 2:73–91
- SRC Consulting (UK) Limited (2007) An independent mineral experts' report on the gold mining and exploration assets of Saudi Arabian Mining Company (Ma'aden)
- Madani A (2002) Selection of the optimum landsat TM bands for lineament extraction, wadi Natash area, South Eastern Desert, Egypt. *Asian Journal of Geoinform* 3:71–76
- Madani A (2009) Utilization of landsat ETM+ data for mapping gossans and iron rich zones exposed at Bahrah Area, Western Arabian shield, Saudi Arabia. *JKAU: Earth Sci* 20(1):35–49
- Madani A (2011) Knowledge-driven GIS modeling technique for gold exploration, Bulghah gold mine area, Saudi Arabia. *The Egyptian Journal of Remote Sensing and Space Sciences* 14:91–97
- Madani A, Emam A (2011) SWIR ASTER band ratios for lithological mapping and mineral exploration: a case study from El Hudi area, southeastern desert, Egypt. *Arab J Geosci* 4(1–2):45–52
- Magowe M, Carr J (1999) Relationship between lineaments and groundwater occurrence in Western Botswana. *Groundwater* 27(2):282–286
- Masoud A, Koike K (2011) Auto-detection and integration of tectonically significant lineaments from SRTM DEM and remotely-sensed geophysical data. *ISPRS J Photogramm Remote Sens* 66(6):818–832
- Morris K (1991) Using knowledge-base rules to map the three dimensional nature of geological features. *Photogramm Eng Remote Sens* 57:1209–1216
- Musumeci G, Ribolini A, Spagnolo M (2003) The effects of late Alpine tectonics in the morphology of the Argentera Massif (Western Alps, Italy–France). *Quat Int* 101–102:191–201
- O'Leary DW, Friedman JD, Pohn HA (1976) Lineaments, linear, lineation: some proposed new standards for old terms. *Bull Geol Soc Am* 87:1463–1469
- Odeyemi I B, Malomo S, Okufarasin Y A (1985) Remote sensing of rock fractures and groundwater development success in parts of southwestern Nigeria. *Natural Resources Forum, United Nations, New York*, 9(4), 311–315
- Quick JE (1991) Late proterozoic transpression of the Nabitah fault system-implications for the assembly of the Arabian shield. *Precambrian Res* 53:119–147
- Ribolini A, Spagnolo M (2008) Drainage network geometry versus tectonics in the Argentera Massif (French–Italian Alps). *Geomorphology* 93:253–266
- Sabins F (1997) *Remote sensing: principles and interpretation*, 3rd edn. Freeman Company, New York
- Solomon S, Ghebream G (2006) Lineament characterization and their tectonic significance using Landsat TM data and field studies in the central highlands of Eritrea. *J Afr Earth Sci* 46:371–378

- Süzen ML, Toprak V (1998) Filtering of satellite images in geological lineament analyses: an application to a fault zone in Central Turkey. *Int J Remote Sens* 19:1101–1114
- Wahby A, Madani A, Khalil D (2001) Automatic extraction of linear features from satellite data using spatial analysis technique. *Egypt J Geol* 45(2):757–766
- Woodruff K D, Talley J H, Miller J C (1974) Selection of sites for high yielding wells in the Delaware, Piedmont area. In: Abstract with programs, Northeastern Section Geological Society of America, Baltimore, Maryland
- Zakir F, Qari M, Mostfa M (1999) A new optimizing technique for preparing lineament density maps. *Int J Remote Sens* 20:1073–1085